Dalton Transactions

ROYAL SOCIETY OF CHEMISTRY

PAPER

Cite this: *Dalton Trans.*, 2021, **50**, 15778

Tetra-substituted phthalocyanines bearing thiazolidine derivatives: synthesis, anticancer activity on different cancer cell lines, and molecular docking studies†

Ahmet T. Bilgiçli, *[a] Ceylan Hepokur, [b] Hayriye Genc Bilgicli, [a] Burak Tüzün, [c] Armağan Günsel, [a] Sema Mısır,[b] Mustafa Zengin[a] and M. Nilüfer Yarasir [a]

In the first step, (4*R*)-2-(2-hydroxyphenyl)thiazolidine-4-carboxylic acid (**c**) and 2-(2-(3,4-dicyanophenoxy)phenyl)thiazolidine-4-carboxylic acid (**1**) were prepared. Then, the peripherally tetra-substituted metallophthalocyanines [ZnPc (**2**), CuPc (**3**), and CoPc (**4**)] were synthesized by using **1**. The structures of the obtained compounds were characterized by common spectroscopic methods. Aggregation behaviors of the tetra-substituted metallophthalocyanines (**2–4**) were investigated by UV-Vis and fluorescence spectroscopy in the presence/absence of soft metal ions. The electronic spectra of the newly synthesized metallophthalocyanines [ZnPc (**2**), CuPc (**3**), and CoPc (**4**)] were analyzed by the Bayliss method. The fluorescence quantum yield of diamagnetic ZnPc (**2**) was obtained in DMSO at room temperature. Also, the anticancer activity of the newly synthesized metallophthalocyanine derivatives was studied on C6, DU-145, and WI-38 cell lines and investigated using six concentrations (3.125; 6.25; 12.5; 50; 75; 100 μg L^{-1}). The cell cycle and apoptosis analyses of CuPc (**3**) were performed. In addition, the chemical and biological activities of 2-(2-(3,4-dicyanophenoxy)phenyl)thiazolidine-4-carboxylic acid (**1**) and its novel type metallophthalocyanines [ZnPc (**2**), CuPc (**3**), and CoPc (**4**)] were compared with many parameters obtained from the Gaussian software and molecular docking methods.

Received 17th June 2021,
Accepted 5th October 2021

DOI: 10.1039/d1dt02023d

rsc.li/dalton

1. Introduction

Cancer is the second most common cause of death worldwide today, increasing due to many reasons such as advancing age, decreased physical activity, harmful habits, smoking, alcohol, and changing diets. In the 2020 World Health Organization report on cancer, the organization estimated that cancer-related deaths in low and middle-income countries will double by 2040 compared to those in 2018. In addition, cancer is the cause of approximately 30% of all premature deaths from non-communicable diseases among adults aged 30–69 years.[1]

It is known that chemotherapy and radiotherapy methods are very effective in cancer treatment. However, the use of these methods is being reduced due to acute toxicities and the ability of tumors to form drug-resistant phenotypes. In addition, treatment success rates are pretty low in the case of late diagnosis in the fight against cancer. For this reason, new treatment methods are being developed, and will increase the success rate of treatment. Therefore, scientists are looking for new drugs and procedures for the treatment of cancer. Recently, photodynamic therapy (PDT) has received widespread attention as an alternative to chemotherapy and radiotherapy.[2]

Phthalocyanines are aromatic macrocyclic compounds that are known as tetrabenzo[5,10,15,20]tetraazaporphyrins. It is well known that the phthalocyanines have unique properties with a conjugated 18 π-electron system. They are of great interest in many application areas such as chemical sensors,[3] gas sensors,[4] solar cells,[5,6] electrochromic materials,[7] nonlinear optics,[8] catalysts for electrochemical reactions,[9] Langmuir–Blodgett films,[10] antioxidants,[11] antimicrobials,[12] and photodynamic therapy.[13,14] Among them, photodynamic therapy is a treatment method that uses certain drugs, called photosensitizing agents, along with light and oxygen to kill cancer cells. The ability of phthalocyanines to generate singlet oxygen makes them promising for photodynamic therapy.[15]

[a]*Department of Chemistry, Sakarya University, 54140Esentepe, Sakarya, Turkey. E-mail: abilgicli@sakarya.edu.tr; Tel: +90(264)2957116*
[b]*Cumhuriyet University, Faculty of Pharmacy, Department of Basic Pharmaceutical Sciences, Division of Biochemistry, Sivas, Turkey*
[c]*Plant and Animal Production Department, Technical Sciences Vocational School of Sivas, Sivas Cumhuriyet University, 58140 Sivas, Turkey*

†Electronic supplementary information (ESI) available. See DOI: 10.1039/d1dt02023d

Therefore, scientists are working on the synthesis of new substituted phthalocyanine derivatives to investigate their anticancer potential.

In recent research, the most critical problem has been to synthesize compounds have strong biological activities such as anti-tumor, antibacterial, anti-oxidative, and anti-viral activities. In these studies, it has been shown that transition metal complexes are more active than their ligand molecules. Synthesizing more effective and active molecules involves many experimental procedures. In addition, these experimental studies are very costly and time-consuming, so some theoretical software packages have been developed, especially in recent years.

The main goal in drug development is always the synthesis of more effective molecules than the previous ones. Studies have shown that transition metal complexes are more active anticancer drugs than the ligand molecules that form them. This leads to a time consuming and costly process. These disadvantages can be eliminated by getting support from the theoretical software developed, especially in recent years.[16,17] As a result, the biological and chemical activities of the synthesized compounds were compared using the Gaussian software and the molecular docking method.

In this work, the synthesis and characterization of 2-(2-(3,4-dicyanophenoxy)phenyl)thiazolidine-4-carboxylic acid (**1**) and its tetra-substituted metallophthalocyanines [ZnPc (**2**), CuPc (**3**), and CoPc (**4**)] were reported. Aggregation behaviors of tetra-substituted metallophthalocyanines containing thiazolidine-4-carboxylic acid derivatives were investigated in solution media. The effect of organic solvents such as DMF, DMSO, and $CHCl_3$ on the UV-Vis spectra of tetra-substituted metalophthalocyanines containing thiazolidine derivatives was investigated. Also, the effect of soft metal ions on aggregation properties was studied in solution media, and the obtained results were interpreted. The fluorescence quantum yield of ZnPc (**2**) was investigated to show the effect on the fluorescence process. The anticancer activity of tetra-substituted metallophthalocyanines containing thiazolidine-4-carboxylic acid derivatives was studied on the different cancer cells. Finally, the newly synthesized compounds' chemical and biological activities (**1–4**) were compared with various parameters obtained from the Gaussian software and molecular docking methods.

2. Experimental

2.1. Materials and methods

The chemical substances and solvents used to synthesize compounds were provided commercially (Merck, Sigma-Aldrich, and Fluka). The Dulbecco's Modified Eagle's Medium (DMEM), phosphate buffer saline (PBS), fetal bovine serum (FBS), and penicillin–streptomycin (PS) were purchased from Gibco (Meckenheim, Germany). The commercial kit XTT (sodium 3-[1-[(phenylamino)-carbonyl]-3,4-tetrazolium]-bis(4-methoxy-6-nitro) benzenesulfonic acid) was obtained from Cayman Chemical Company. Trypsin was purchased from Biological Industries. ^{1}H and ^{13}C-NMR spectra were recorded using a Varian 300 MHz Mercury Plus instrument using TMS as the internal standard. The PerkinElmer Spectrum Two FT-IR (ATR sampling accessory) spectrometer was used to measure vibrational spectra. The electronic spectra of the compounds were recorded by using an Agilent Model 8453 diode array ultraviolet-visible (UV-Vis) spectrophotometer. Fluorescence spectra were recorded by using a Hitachi S-7000 fluorescence spectrophotometer.

2.2. Synthesis

2.2.1 Synthesis of (4*R*)-2-(2-hydroxyphenyl)thiazolidine-4-carboxylic acid. (4*R*)-2-(2-Hydroxyphenyl)thiazolidine-4-carboxylic acid (**c**) was prepared according to the literature.[18] 2-hydroxybenzaldehyde (**b**) (10 mmol) was dissolved in EtOH (10 ml). To the solution was added L-cysteine hydrochloride (**a**) (1.57 g, 10 mmol) and NaOAc (0.98 g, 12 mmol) dissolved in water (10 ml). The reaction mixture was then stirred for 24 hours at room temperature. The precipitate was then separated by filtration, and washed several times with EtOH (Scheme 1). ^{1}H NMR (300 MHz, DMSO-d_6) 3.05–2.94 (m, 1H^a, 1H^b), 3.21 (dd, 1H^a, *J* 6.8, 10.2 Hz), 3.34 (dd, 1H^b, *J* 6.9, 9.4 Hz), 3.83 (dd, 1H^a, *J* 6.9, 8.9 Hz), 4.21 (dd, 1H^b, *J* 5.2, 6.8 Hz), 5.65 (s, 1H^b), 5.84 (s, 1H^a), 6.73–6.83 (m, 2H^a,2H^b), 7.06 (td, 1H^a,1H^b, *J* 7.6, 1.7 Hz), 7.13 (td, 1H^a,1H^b, *J* 7.7, 1.7 Hz), 7.30 (d, 1H^a,1H^b, *J* 7.7 Hz), 7.34 (dd, 1H^a,1H^b, *J* 1.7, 7.7 Hz), 9.83 (s, 2H, –OH^a, –OH^b) (Fig. S1†). ^{13}C NMR (75 MHz, DMSO) δ: 173.6, 173.1, 155.8, 155.2, 129.7, 128.8, 128.6, 128.3, 126.7, 124.9, 119.7, 119.4, 116.3, 115.7, 68.3, 66.3, 65.9, 65.5, 38.8, 37.8.

2.2.2. The synthesis of 2-(3-(3,4-dicyanophenoxy)phenyl) thiazolidine-4-carboxylic acid (1). (4*R*)-2-(2-Hydroxyphenyl)thiazolidine-4-carboxylic acid (1.1 g, 4.88 mmol) dissolved in DMF (10 ml), and anhydrous K_2CO_3 (5.36 g, 38.88 mmol) were stirred at room temperature (≈25 °C) for 15 minutes. Then, 4-nitrophthalonitrile (1.0 g, 5.78 mmol) dissolved in DMF was added to the reaction vessel drop by drop. The reaction mixture was stirred at 40 °C for 48 h. TLC was used for checking the completion of the reaction. After the reaction was completed, the reaction mixture was cooled at room temperature (≈25 °C) and poured into ice water. The product was precipitated after adding some acid (2–3 drops of concentrated HCl) to the medium. The obtained product was filtered and washed with water several times. Further purification was performed by chromatography over a silica gel column using an eluent of $CHCl_3$ (Scheme 1).

2-(3-(3,4-Dicyanophenoxy)phenyl)thiazolidine-4-carboxylic acid (**1**) is soluble in organic solvents such as $CHCl_3$, THF, DMSO and DMF. Yield of (**2**): 1.16 g (75%). Anal. Calcd for $C_{18}H_{13}N_3O_3S$ (351.38 g mol^{-1}): C, 61.53; H, 3.73; N, 11.96; Found: C, 62.15; H, 3.69; N, 12.08. FT-IR (ν_{max}/cm^{-1}): 3280 (carboxylic acid OH), 3094, 3060, 3022 (H-Aromatic), 2230 (C≡N), 1678 (C=O), 1577(Aromatic C=C), 1460, 1380, 1244, 1213, 755, 522. ^{1}H NMR (300 MHz, DMSO-d_6) δ 8.08 (s, 1H^a), 7.96 (d, *J* = 8.4 Hz, 1H^a), 7.76 (dd, *J* = 8.4 Hz, 1H^a), 7.51

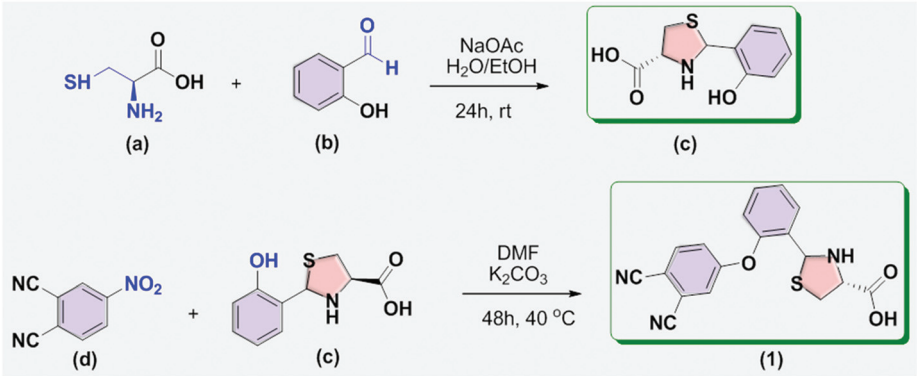

Scheme 1 Synthetic route of 2-(2-(3,4-dicyanophenoxy)phenyl)thiazolidine-4-carboxylic acid (**1**).

(d, J = 7.8 Hz, 1H^b), 7.38 (d, J = 8.2 Hz, 1H^b), 7.30 (d, J = 7.5 Hz, 1H^b), 7.20 (d, J = 7.7 Hz, 1H^a), 7.05 (dt, J = 24.2, 7.6 Hz, 3H^a), 6.86–6.64 (m, 4H^b), 5.86 (s, 1H^a), 5.60 (s, 1H^b), 3.89 (dd, J = 6.5 Hz, 1H^a, 1H^b), 3.13 (dd, J = 10.0, 6.5 Hz, 1H^a,1H^b), 2.96–2.72 (m, 1H^a, 1H^b) (Fig. S2†). MALDI-MS: m/z: 352.514 $[M + H]^+$, 435.623 $[M + K + 2Na–2H]^+$.

2.2.2. General procedure for the synthesis of metallophthalocyanines (2–4). The tetra-substituted metallophthalocyanines containing thiazolidine-4-carboxylic acid derivatives [ZnPc (**2**), CuPc (**3**), and CoPc (**4**)] were prepared by the cyclotetramerization reaction of compound (**1**) in the presence of zinc acetate or copper chloride or cobalt chloride salts in n-hexanol/DBU media. 2-(3-(3,4-dicyanophenoxy)phenyl)thiazolidine-4-carboxylic acid (**1**) (100 mg, 0.28 mmol) was stirred at 140 °C temperature for 5 h under a N_2 atmosphere in hexanol and 1,8-diazabicyclo[5.4.0] undec-7-ene (DBU, 0.05 ml) media in the presence of anhydrous metal salts [($Zn(CH_3COO)_2$, $CuCl_2$ and $CoCl_2$]: ~(0.030 g, excess) (Scheme 2). The yellow products were obtained, and they were precipitated with hexane, then afterward, washed with cold MeOH several times. The further purification of the obtained phthalocyanine derivatives was performed by column chromatography using CH_2Cl_2 as an eluent. Finally, the obtained new metallophthalocyanines [ZnPc (**2**), CuPc (**3**), and CoPc (**4**)] are soluble in DMF, DMSO, and $CHCl_3$.

Yield of compound (**2**): 33.5 mg (32%). Chemical formula of (**2**): $C_{72}H_{52}N_{12}O_{12}S_4Zn$ (1470.93 g mol^{-1}). Elemental analysis of compound (**2**) (%), calculated: C (58.79), H (3.56), N (11.43) O (13.05), S (8.72) Zn (4.45), found: C (58.96) H (3.51), N(11.76). UV-Vis (DMSO) λ_{max}/nm: 692 (Q-band), 623 (vibrational satellite), 309 (B-band). FT-IR ν/cm^{-1}: 3216 (carboxylic acid OH), 3040, 3016 (H-aromatic), 1673 (C=O), 1584 (aromatic C=C), 1444, 1389, 1244, 1092, 750. ^{1}H-NMR (d-DMSO, δ ppm): 8.46–8.25 (m, 12H), 8.16–7.95 (m, 16H), 5.65 (s, 4H), 5.86 (s, 4H), 4.20 (m, 8H), 3.20–3.0 (m, 4H). 1472.01 $[M + H]^+$ and 1541.12 $[M + 3Na + H]^+$.

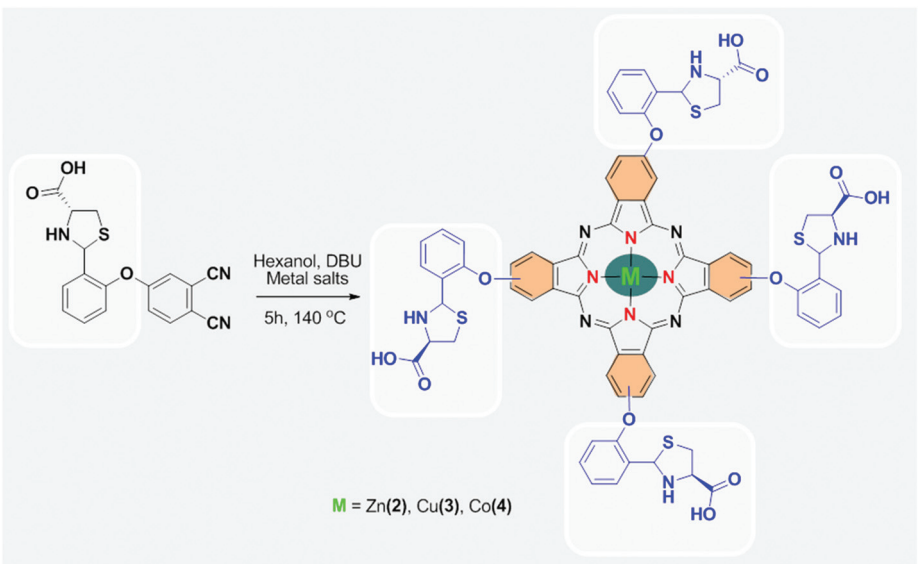

Scheme 2 Synthetic route of the novel metallophthalocyanines [ZnPc (**2**), CuPc (**3**), and CoPc (**4**)].

Yield of compound (**3**): 32 mg (30%). Chemical formula of (**3**): $C_{72}H_{52}N_{12}O_{12}S_4Cu$ (1469.06 g mol^{-1}). Elemental analysis of compound (**3**) (%), calculated: C (58.87), H (3.57), Cu (4.33), N (11.44) O (13.07), S (8.73), found: C (59.05) H (3.52), N (11.66). UV-Vis (DMSO) λ_{max}/nm: 690 (Q-band), 621 (vibrational satellite), 314 (B-band). FT-IR ν/cm^{-1}: 3216 (carboxylic acid OH), 3088, 3056, 3032 (H-aromatic), 1671 (C=O), 1581 (Aromatic C=C), 1452, 1382, 1242, 1213, 1108, 753. MALDI-MS: *m*/*z*: 1470.53 $[M + H]^+$ and 1516.21 $[M + 2Na + H]^+$.

Yield of compound (**4**): 26 mg (25%). Chemical formula of (**4**): $C_{72}H_{52}N_{12}O_{12}S_4Co$ (1463.20 g mol^{-1}). Elemental analysis of compound (**4**) (%), calculated: C (59.05), H, (3.58), Co, (4.02), N (11.48), O (13.11), S (8.76), found: C (59.39), H (3.50), N (11.61). UV-Vis (DMSO) λ_{max}/nm: 693 (Q-band), 625 (vibrational satellite), 304 (B-band). FT-IR ν/cm^{-1}: 3249 (carboxylic acid OH), 3106, 3048 (H-aromatic), 1678 (C=O), 1582 (aromatic C=C), 1436, 1348, 1236, 1188, 1132, 747. MALDI-MS: *m*/*z*: 1464.82 $[M + H]^+$ and 1488.35 $[M + Na + H]^+$.

2.3. Fluorescence quantum yields

The comparative method was used to determine the fluorescence quantum yields (Φ_F) of the phthalocyanine complexes using the below eqn (1).[19]

$$\Phi_F = \Phi_F(\mathrm{Std})\frac{F \cdot A_{Std} \cdot n^2}{F_{Std} \cdot A \cdot {n_{Std}}^2} \quad (1)$$

F and F_{std} are the areas under the fluorescence curves of the complexes and the standard, respectively. A and A_{std} are the respective absorbances of the sample and standard compounds at the excitation wavelength. n and n_{std} are the refractive indices of the used solvents, respectively. Un-substituted ZnPc was used as a standard in DMSO where $\Phi_F = 0.20$.[20]

2.4. Biological study

2.4.1. Determination of total antioxidant status (TAS). A commercial kit manufactured by Rel Assay Diagnostics was used to determine the total antioxidant status. According to this method, the antioxidants in the sample are reduced from the dark blue-green ABTS radical form to the colorless reduced ABTS form. The change in the absorbance at 660 nm is related to the total antioxidant capacity of the sample. The assay was calibrated with the reference substance used as the stable standard antioxidant solution, which is the vitamin E analog and called the Trolox equivalent. The TAS measurement was performed according to the kit procedure. After calculating the difference between the absorbances, the TAS value is calculated according to eqn (2).[21]

$$\Delta A = x = \frac{\Delta A(\mathrm{sample})}{\Delta A(\mathrm{standard})} \times 20 \quad (2)$$

2.4.1.1 Cell lines. Rat glioma cancer (C6), human prostate carcinoma (DU-145), and normal human lung fibroblast (WI-38) cell lines were generously provided by the Hepokur cancer research laboratory Sivas Cumhuriyet University, Sivas, Turkey. Cells were cultured in DMEM (high glucose) supplemented with 10% fetal bovine serum (FBS), 1% L-glutamine, 100 IU mL^{-1} penicillin and 10 mg mL^{-1} streptomycin in a 95% humidity and 5% CO_2 incubator at 37 °C.

2.4.2. *In vitro* photodynamic therapy. For photodynamic therapy experiments, healthy and cancer cell lines were incubated in 24-well plates with different concentrations (0–100 μg L^{-1}) of Zn, Cu, and Co metal phthalocyanine compounds for 2 hours. After incubation for 2 h, a red diode laser (fluence 4.5 J cm^{-2}, power density 114.60.10^{-3} MW cm^{-2}) was applied to each well with a light source of 90 mW and a 1 cm radius of the light source (660 nm, the 40 s) (Cube System, Coherent). All these processes were carried out at room temperature in the dark.

2.4.3. Cytotoxic tests

2.4.3.1. Determination of the IC_{50} dose of the compounds in cancer cell lines. The IC_{50} value of the synthesized organic compounds, which kills half of the cells, was determined at the end of the process. Sterile 96-well plates were seeded with 10×10^4 cells per well. The cells were counted using the Olympus R1 cell counter. The compounds were applied to these wells at different concentrations (100–50–25–12.5–6.25–3.125 μg L^{-1}). At the end of the determined incubation times, the compounds were removed from the wells, and the XTT (2,3-bis(2-methoxy-4-nitro-5-sulfophenyl)-5-[(phenylamino)carbonyl]-2*H*-tetrazolium hydroxide) kit was applied.

2.4.4. Cell cycle analysis. The cell cycle analysis was performed by flow cytometry in DU-145 cells which were treated with 3.28 μg L^{-1} of CuPc (**3**) for 24 h. Then, all cells were collected and centrifuged for 5 min at 300*g* at 25 °C. 250 mL of trypsin buffer was added to each tube and incubated at 25 °C for 10 min. After 10 min, 200 mL of the trypsin inhibitor and RNase buffer were added to the mixture, which was again incubated for 10 min. 200 μL of the cold PI stain solution was added to each tube, and data from 3×10^4 cells were measured. All data were compared with those of the untreated control cells.

2.4.5. Apoptosis analysis. Apoptosis analysis was performed by flow cytometry in DU-145 and WI-38 cells. In this analysis, we used a commercial kit (BD Pharmingen™, Cat. no: 559763, San Diego, CA, USA) following the manufacturer's recommendations. DU-145 and WI-38 cells were treated with 3.28 μg L^{-1} concentration of CuPc (**3**) for 24 h, then collected and washed twice with ice-cold PBS. To the cells, pellets were added and 100 μL 1× binding buffer was added to each tube. After that 5 μL of FITC Annexin V and 5 μL of PI were added to each tube, and all mixtures were incubated for 15 min in the dark at 25 °C. Data from 1×10^4 cells were harvested and analyzed. The results were compared with those of the untreated negative control cells.

2.5. Theoretical methods

2.5.1. Gaussian study. Some methods are used to obtain information about the biological and chemical activities of compounds. Among these, the most commonly used theoretical methods are DFT and docking calculations. These methods provide excellent convenience for comparing the

activities of the compounds. In this study, GaussView 5.0.8, Gaussian09 AS64L-G09RevD.01, ChemDraw Professional 15.1, and Chemcraft V1.8 package programs were used in the preparation of molecules.[22–25] Theoretical results were obtained by the Hartree–Fock (HF),[26,27] Lee–Yang–Parr (B3LYP),[28,29] and M06-2X[30] methods with 3-21G, 6-31G, and sdd basis sets. As a result of the calculations made on these basis sets, many parameters can be obtained, and are called quantum chemical parameters such as E_{HOMO}, E_{LUMO}, ΔE (HOMO–LUMO energy gap), electronegativity (χ), chemical potential (μ), chemical hardness (η), electrophilicity (ω), nucleophilicity (ε), global softness (σ) and proton affinity (PA).[31–34] HOMO is the highest occupied molecular orbital, and LUMO is the lowest unoccupied molecular orbital. The HOMO and LUMO values are used to get information about the activities of the molecules by using these methods.

$$\mu = -\chi = \left(\frac{\partial E}{\partial N}\right)_{\nu(r)} \quad (3)$$

$$\eta = \frac{1}{2}\left(\frac{\partial^2 E}{\partial N^2}\right)_{\nu(r)} = \frac{1}{2}\left(\frac{\partial \mu}{\partial N}\right) \quad (4)$$

Ionization energy (I) and electron affinity (A) of the studied molecules are calculated with the HOMO and LUMO energies, that are involved in electronegativity, global softness, and chemical hardness, which were obtained by the following equations.[35]

$$\chi = -\mu = \left(\frac{I + A}{2}\right) \quad (5)$$

$$\eta = \frac{I - A}{2} \quad (6)$$

It is well known that global softness is defined as the inverse of the chemical hardness.

$$\sigma = 1/\eta \quad (7)$$

$$\chi = -\mu = \left(\frac{-E_{HOMO} - E_{LUMO}}{2}\right) \quad (8)$$

$$\eta = \left(\frac{E_{LUMO} - E_{HOMO}}{2}\right) \quad (9)$$

The global electrophilicity index[36] (ω) that is investigated by Parr *et al.* is the inverse of nucleophilicity and is calculated by eqn (10). Electrophilicity and nucleophilicity are used for the prediction of organic and inorganic reaction mechanisms. Nucleophilicity (ε) is defined as the inverse of the electrophilicity in eqn (11).

$$\omega = \mu^2/2\eta = \chi^2/2\eta \quad (10)$$

$$\varepsilon = 1/\omega \quad (11)$$

2.5.2. Docking study. The molecular docking method was used to contribute to a better understanding of the biological activities of the new compounds [(**1**), ZnPc (**2**), CuPc (**3**), and CoPc (**4**)].[16] In the docking study, the biological activity values of the compound (**1**) and its phthalocyanine derivatives [ZnPc (**2**), CuPc (**3**), and CoPc (**4**)] against human galectin-8, brain cancer cells, and protease cancer cells were compared. *.pdb extension files were obtained by using the optimized structures obtained from the Gaussian software program.[37] Cancer tissues and molecule files were studied using HEX 8.0.0.[38] For docking displays, help was received from the SeeSar 9.0 software program.[39]

3. Results and discussion

3.1. Spectroscopic characterization of novel type phthalocyanines

The structure of the tetra-substituted metallophthalocyanines containing thiazolidine-4-carboxylic acid derivatives [ZnPc (**2**), CuPc (**3**), and CoPc (**4**)] was characterized by the combination of some spectroscopic techniques such as FT-IR, ^{1}H-NMR, and UV-Vis spectroscopy. The obtained spectra were found to be compatible with the related structures. Four isomer-mixed products are obtained in the synthesis of phthalocyanines, and they may not be able to separate by column chromatography easily. The four isomer mixtures of phthalocyanines could not be separated by the column method. Therefore, the obtained spectra of the novel type metallophthalocyanines (ZnPc (**3**), CuPc (**4**), and CoPc (**5**)) are a mixture of four isomers.[40]

Infrared spectroscopy is a simple and useful technique for the characterization of the synthesized compounds. It is well known that 4-nitrophthalonitrile used as the starting material in this study shows characteristic peaks at 1532 cm^{-1} and 1350 cm^{-1} due to the nitro groups and at 2220 cm^{-1} due to C≡N vibration.[41] The novel phthalonitrile derivative 2-(3-(3,4-dicyanophenoxy)phenyl)thiazolidine-4-carboxylic acid was obtained by the nucleophilic aromatic substitution reaction between 4-nitrophthalonitrile and (4*R*)-2-(3-hydroxyphenyl) thiazolidine-4-carboxylic acid. Characteristic peaks at 1532 cm^{-1} and 1350 cm^{-1} related to the nitro groups were not observed in the infrared spectrum after the reaction was completed. The peak of the –C≡N vibration at 2220 cm^{-1} shifted to 2242 cm^{-1} for the 2-(3-(3,4-dicyanophenoxy)phenyl)thiazolidine-4-carboxylic acid. Aromatic CH peaks at 3097 cm^{-1}, 3061 cm^{-1} and 3022 cm^{-1} and carbonyl stretch (C=O) at 1655 cm^{-1} were observed for 2-(3-(3,4-dicyanophenoxy)phenyl) thiazolidine-4-carboxylic acid. In the infrared spectra recorded after the synthesis of new metal phthalocyanines, the peak at 2242 cm^{-1} of the C≡N vibration has disappeared (Fig. S3†). This could be the evidence of a cyclotetramerization reaction.

^{1}H-NMR spectroscopy was used for the characterization of the synthesized compounds. The ^{1}H-NMR spectra of new phthalonitrile 2-(3-(3,4-dicyanophenoxy)phenyl)thiazolidine-4-carboxylic acid and its zinc metallophthalocyanine ZnPc (**2**) were obtained in deuterated dimethyl sulphoxide solution. The ^{1}H-NMR spectra of copper metallophthalocyanine CuPc (**3**) and cobalt metallophthalocyanine CoPc (**4**) could not be recorded due to the paramagnetic nature of copper and cobalt

ions.[42] The aromatic protons of ZnPc (2) could be recorded as broad peaks due to the phthalocyanine's conjugated 18 π-electron system.

It is well known that the electronic spectra of the phthalocyanines are one of the essential properties. Their spectral properties are due to the aromatic cyclic conjugated 18 π-electron system, and they show characteristic peaks called Q- and B-bands in their electronic spectra. The Q-band appears at 650–700 nm due to the π–π* transition and the B band appears at 300–400 nm due to the deeper π–π* transition. Therefore, UV-Vis spectroscopy is routinely used for the characterization of phthalocyanines.[43] The Q-bands of the novel type metallophthalocyanines [ZnPc (2), CuPc (3), and CoPc (4)] appeared at 692 nm, 690 nm, and 693 nm as a single band, respectively (Table 1). The B-bands of related metallophthalocyanines (ZnPc (3), CuPc (4), CoPc (5)) were observed at 309 nm, 314 nm, and 304 nm, respectively (Fig. 1). The Q and B-band values are compatible with the literature values of newly synthesized metallophthalocyanines bearing thiazolidine groups in peripheral positions.

3.2. Aggregation studies

Phthalocyanines are known to exhibit aggregation properties. It is difficult to predict what causes the aggregation of phthalocyanines due to the influence of many factors such as conjugated 18 π-electron systems, solvents, concentration, the central metal, axial substituents on the central metal, the nature of the functional group, and temperature.[44] However, the aggregation tendency of phthalocyanines can be reduced by changing these properties. UV-Vis spectroscopy is a very simple and useful technique that can be used to study the aggregation phenomena of phthalocyanines because the aggregation behavior of phthalocyanines primarily affects the Q bands. Therefore, the aggregation behavior of the newly synthesized metallophthalocyanines was investigated by UV-Vis spectrophotometry.

The UV-Vis spectrum of the newly synthesized metallophthalocyanines at different concentrations was recorded in DMSO. When the concentration of the metallophthalocyanines was increased, the intensity of the Q bands, which appeared at 692 nm, 690 nm, and 694 nm, also increased. The new band formation and blue/redshift were not observed (Fig. S4 for (2), Fig. 2 for (3), and Fig. S5† for (4)). When the graphs obtained

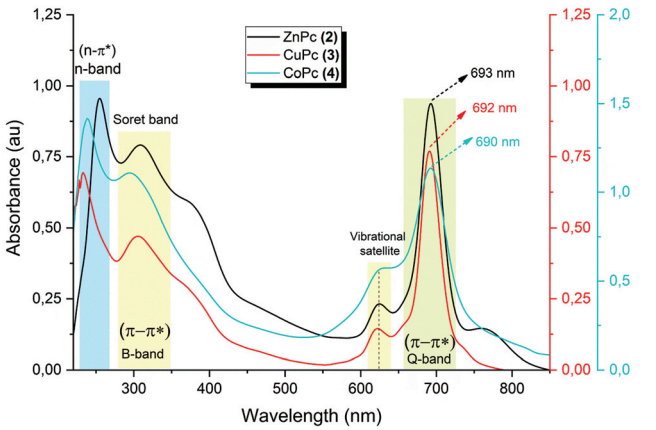

Fig. 1 UV-Vis spectra of the novel metallophthalocyanines [ZnPc (3), CuPc (4), and CoPc (5)] in DMSO at room temperature.

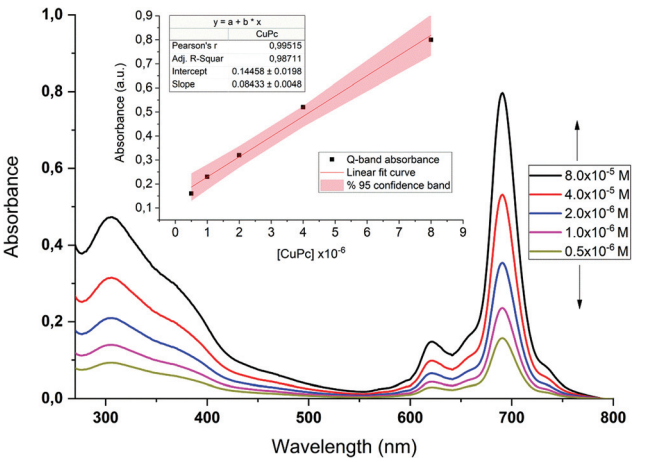

Fig. 2 UV-Vis spectra of CuPc (3) at different concentrations in DMSO at room temperature (inset: the plot of Q band absorbance *versus* concentration).

Table 1 UV-Vis and fluorescence data of the novel metallophthalocyanines (2–4)

	UV-Vis		Fluorescence			
Compound	λ_{abs} (nm)	log ε/cm^{-1} mol^{-1} L	λ_{em} (nm)	λ_{ex} (nm)	Stokes shift	Φ_F
ZnPc (2)	692	4.67	703	691	11	0.13
CuPc (3)	690	4.59	—	—	—	—
CoPc (4)	693	4.74	—	—	—	—
ZnPc[a]	672[a]		672[a]	682[a]	10[a]	0.20[a]

[a] The values were obtained from ref. 19.

are examined, it can be concluded that the newly synthesized metallophthalocyanines bearing thiazolidine groups in peripheral positions are non-aggregated in DMSO.

In the present study, the electronic spectra of the novel type metallophthalocyanines [ZnPc (2), CuPc (3), and CoPc (4)] have also been analyzed by the Bayliss method in the DMF, DMSO, and $CHCl_3$ solvents. The frequency of the Q-band maximum of the novel type metallophthalocyanines was plotted against $f(n) = (n^2 - 1)/(2n^2 + 1)$. "$n$" in this function is the refractive index of the used solvents. For the novel type metallophthalocyanines, a more red-shifted Q-band maximum was obtained in the DMSO solvent, while a shorter-wavelength maximum was obtained in DMF (Fig. S6 for ZnPc (3), Fig. 3 for CuPc (4), and Fig. S7† for CoPc (5)). When these graphs were examined, the change in the frequencies of the Q-band maxima was obtained linearly. A linear correlation of the novel type metallophthalocyanines in the DMF, DMSO, and $CHCl_3$ solvents indicates that the red shifts in the electronic spectra are mainly due to

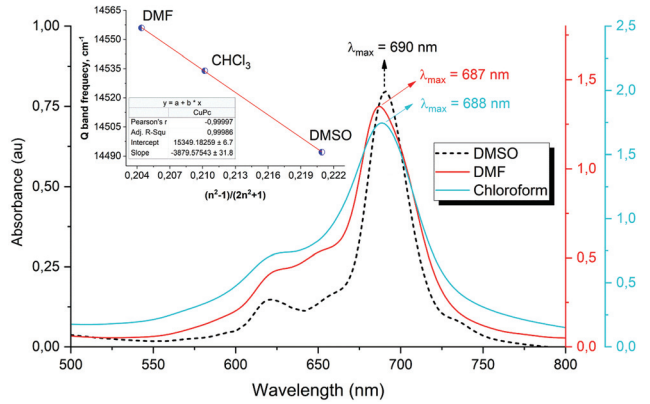

Fig. 3 UV-Vis spectra of CuPc (**3**) in different solvents (inset: the plot of the Q band frequency of CuPc (**3**) against $(n^2 - 1)/(2n^2 + 1)$).

the solvation effect. Also, this shows that the coordination effect of the solvents is small.

3.3. Metal ion binding studies

The sensitivity behaviors of 2-(2-hydroxyphenyl)thiazolidine-4-carboxylic acid (**c**) were investigated by UV-Vis spectroscopy and fluorescence spectroscopy in the presence of some metal ions such as K^+, Ag^+, Ca^{2+}, Mg^{2+}, Mn^{2+}, Mg^{2+}, Pb^{2+}, Zn^{2+}, Fe^{2+}, Hg^{2+}, Pd^{2+} Ni^{2+}, and Cu^{2+} in our previous study. According to the results obtained from that study, the functional group 2-(2-hydroxyphenyl)thiazolidine-4-carboxylic acid is optically sensitive to Pd^{2+}, Cu^{2+} and Zn^{2+} ions.[45] Also, it is well known that substituted phthalocyanines with suitable functional groups might be optically sensitive towards valuable metal ions such as Ag^+ and Pd^{2+}.[46] Therefore, the optical sensitivity properties of the novel type metallophthalocyanines bearing thiazolidine groups in peripheral positions (**2–4**) were investigated by UV-Vis spectroscopy. According to the UV-Vis results obtained, the substituted phthalocyanines with thiazolidine groups are optically sensitive towards Ag^+ ions. However, the novel type metallophthalocyanines (**2–4**) are not optically sensitive to other metal ions studied in the present work.

Phthalocyanines generally tend to show H-type aggregation in solution media due to the regularity of push and pull forces in H-aggregation. Other factors affecting aggregation can be listed as temperature, concentration, nature of the additive, and the effect of the substituted group. However, J-type aggregation occurs less frequently compared to H-type aggregation. It is important for applications such as photodynamic therapy that the Q-band shifts to red in J-type aggregation. Therefore, the aggregation behavior of the synthesized phthalocyanines when the Ag^+ ion was doped was investigated in solution media at room temperature.

The effect of metal ions on the novel type metallophthalocyanines (**2–4**) was studied by absorbance changes in the UV-Vis spectra during titration with metal ions. Each titration experiment was performed by stepwise addition of dissolved metal salts into the phthalocyanines. The concentration of the metal salts and phthalocyanines was chosen as 10^{-3} mol L^{-1} and 10^{-5} mol L^{-1} to eliminate the absorption decreases due to dilution, respectively. During the titration of the novel type metallophthalocyanines (**2–4**) with Ag^+ ions, the Q band intensity due to monomeric species formed at 692 nm for (**2**), 690 nm for (**3**), and 693 nm for (**4**) decreased and shifted to 764 nm, 720 nm, and 715 nm, respectively (Fig. S8 for (**2**), Fig. 4 for (**3**) and Fig. S9† for (**4**)). The titration of the novel type metallophthalocyanines (**2–4**) with Ag^+ ions caused J-type aggregation.

3.4. Fluorescence studies

The fluorescence behavior and fluorescence quantum yield of ZnPc (**2**) were examined in DMSO at room temperature. The obtained data of ZnPc (**2**) are given in Table 1. The fluorescence excitation and emission spectra of CuPc (**3**) and CoPc (**4**) were not recorded due to the paramagnetic properties of Cu^{2+} and Co_2^+ ions in the Pc core.[47] The absorption, excitation, and emission spectra of ZnPc (**2**) are given in Fig. 5. The Q-band absorption value of ZnPc (**2**) was observed at 692 nm in the excitation spectrum (λ_{Exc} = 650 nm). The emission peak of ZnPc (**2**) appeared at 703 nm upon excitation at 650 nm. As seen in Fig. 5, the fluorescence excitation spectrum is similar to the absorption spectrum, and also, the fluorescence emission spectrum of ZnPc (**2**) is the mirror image of the excitation spectra. Therefore, we can say that the ground and excited states are not affected by excitation. The Stokes shift of ZnPc (**2**) is 11 nm. This value is compatible with those of unsubstituted ZnPc derivatives.

The fluorescence quantum yield (Φ_F) of ZnPc (**2**) was calculated according to the compared method in the literature. The unsubstituted ZnPc was used as a standard compound. The fluorescence quantum yield of unsubstituted ZnPc (ΦF_{Std}) is 0.20.[48] The fluorescence quantum yield (Φ_F) of ZnPc (**2**) was found to be 0.13. The fluorescence quantum yield of ZnPc (**2**) was lower than that of standard unsubstituted ZnPc.

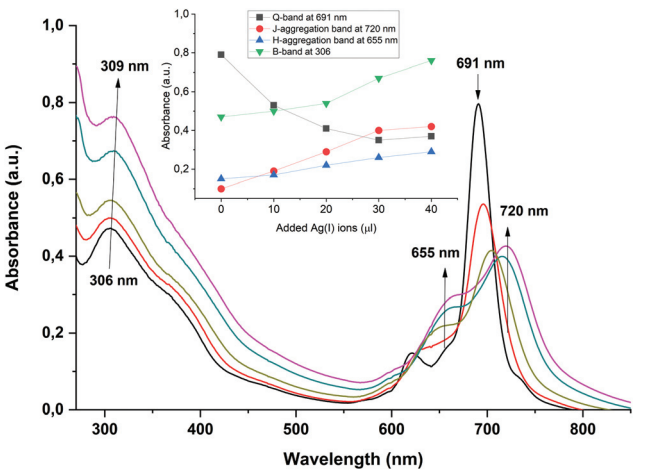

Fig. 4 UV-Vis spectra of CuPc (**3**) during the titration with Ag(I) ions (inset: the plot of Q, B H-aggregation and J-aggregation band absorption values *versus* the amount of Ag(I) ions).

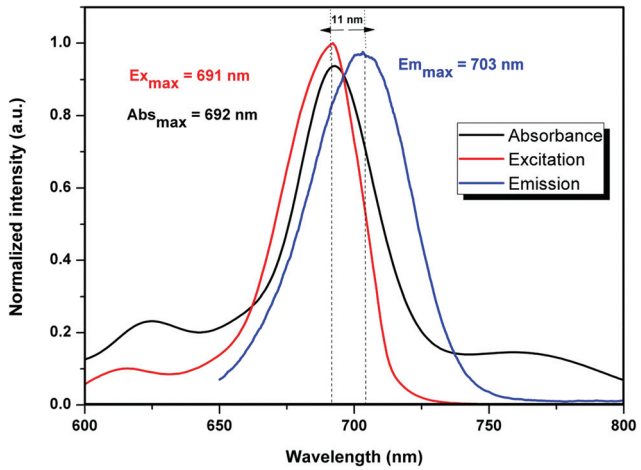

Fig. 5 Absorbance, excitation, and emission spectra of ZnPc (**2**) (λ_{exc} = 600 nm).

Therefore, it can be said that the 2-(3-hydroxyphenyl)thiazolidine-4-carboxylic acid in the peripheral positions of ZnPc (**2**) caused a decrease in the fluorescence quantum yield.

The effect of Ag^{+} ions on the fluorescence properties of ZnPc (**2**) was also investigated by fluorescence emission spectroscopy. The fluorescence emission spectra of ZnPc (**2**) were recorded with the addition of Ag^{+} ions into the DMSO mixture at room temperature. Firstly, the fluorescence emission intensity of ZnPc (**2**) slowly increased with the addition of Ag^{+} ions and shifted from 703 nm to 697 nm. Then, the addition of Ag^{+} ions into ZnPc (**2**) caused fluorescence quenching (Fig. 6).

3.5. Biological results

In this study, we showed that the novel type metallophthalocyanines [ZnPc (**2**), CuPc (**3**), and CoPc (**4**)] have anticancer activity on C6, and DU-145 cells. The IC_{50} values of the complexes on all cells are summarized in Table 2. According to the obtained results, the newly synthesized phthalocyanine derivatives [ZnPc (**2**), CuPc (**3**), and CoPc (**4**)] showed promising anticancer activity against the tested DU-145 cells compared to C6 cells. The ZnPc (**2**) compound exhibits a highly selective cytotoxic effect, especially on DU-145 and C6 cells. The synthesized novel type metallophthalocyanine compounds (**2–4**) might be potentially useful in cancer treatment.

Table 2 IC_{50} values of the novel metallophthalocyanine compounds in cell lines

IC_{50} (μg mL^{-1})	ZnPc (**2**)	CuPc (**3**)	CoPc (**4**)
DU-145	4.74 ± 0.026	3.28 ± 0.041	5.02 ± 0.017
C6	11.16 ± 0.87	19.53 ± 1.12	22.84 ± 1.03
WI	12.30 ± 0.87	28.68 ± 1.65	19.29 ± 1.54

Total antioxidant capacity values greater than or equal to 2.0 are considered to be high.[21] The total antioxidant capacity values of the novel type metallophthalocyanines [ZnPc (**2**), CuPc (**3**), and CoPc (**4**)] are 5.92, 3.94, and 1.37, respectively. The antioxidant capacity of ZnPc (**2**) was found to be the highest among the synthesized novel type metallophthalocyanine compounds with a 5.92 value (Table 3).

3.6. Cell cycle and apoptosis results

The accumulated evidence has shown that a lot of studies have focused on apoptosis and cell cycle arrest for cancer treatment.[49,50] The cell cycle is the process that occurs in the cell that is stimulated for proliferation, and a series of transient biochemical activities are observed.[51] The G1/S checkpoint

Table 3 Total antioxidant (TAS) values

	ZnPc (**2**)	CuPc (**3**)	CoPc (**4**)
(mmol Trolox Equiv. per L)	5.92	3.94	1.37

Table 4 Effect of CuPc (**3**) on cell cycles in DU-145 cells

	G1 phase (%)	S phase (%)	G2/M phase (%)
CuPc (3.28 μg L^{-1})	17.4 ± 1.6	56.5 ± 2.4	26.1 ± 2.02

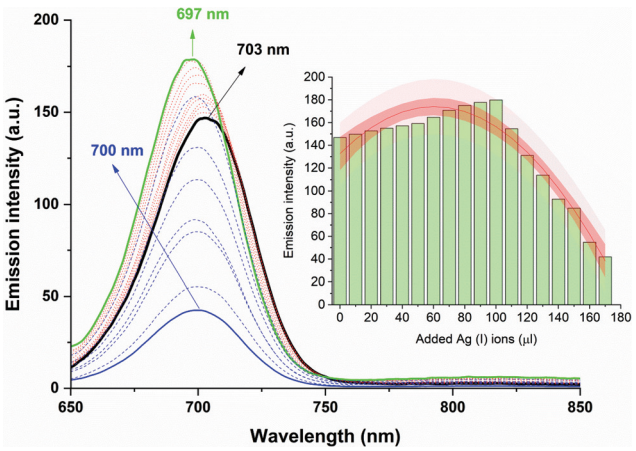

Fig. 6 The fluorescence emission change of ZnPc (**2**) during the titration with Ag^{+} ions (inset: the change of maximum emission intensity during the titration).

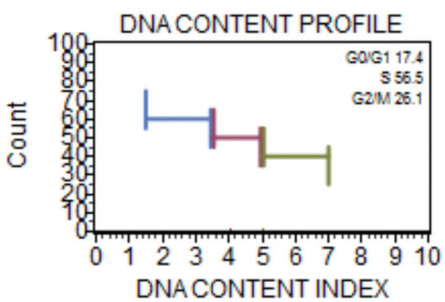

Fig. 7 Flow cytometric analysis of the effects of CuPc (**3**) for 24 h on the cell cycle distribution in DU-145 cells.

is the most critical point for transporting molecules to the nucleus and control of cell proliferation.[52] Apoptosis, or programmed cell death, is a natural process that usually takes place in all tissues to maintain homeostasis and eliminate damaged or unwanted cells.[53]

The cell cycle analysis was performed by flow cytometry in DU-145 cells which were treated with 3.28 μg L^{-1} of CuPc (**3**) for 24 h. The effect of CuPc (**3**) on cell cycle analysis results is presented in Table 4 and Fig. 7. Fig. 7 shows that CuPc (**3**) induced the S phase cell cycle arrest within 24 h.

Apoptosis analysis of CuPc (**3**) was performed by flow cytometry in DU-145 and WI-38 cells. The obtained data of apoptosis analysis are shown in Table 5 and Fig. 8. When Table 5 and Fig. 8 are examined, the novel type copper phthalocyanine (CuPc (**3**)) caused a significant increase in the number of apoptotic cells and reduced the number of viable cells in DU-145 cells. However, CuPc (**3**) did not cause a significant reduction in the number of viable cells in WI-38 cells. While CuPc (**3**) had a great effect on DU145 cells, no significant effect was observed on WI-38 cells. These results suggested that CuPc (3.28 μg mL^{-1}) arrested the cells at the S-phase of the cell cycle and increased the apoptosis in DU-145 cells.

Table 5 The apoptosis analysis of CuPc (**3**) treated DU-145 and WI-38 cells

	Non-apoptotic (%)	Early apoptotic (%)	Late apoptotic (UR)	Necrotic (%)
DU-145 cells	52.71 ± 1.6	2.96 ± 3.5	43.10 ± 3.1	1.24 ± 0.8
WI-38 cells	92.93 ± 2.7	4.55 ± 2.3	1.92 ± 1.9	0.61 ± 0.6

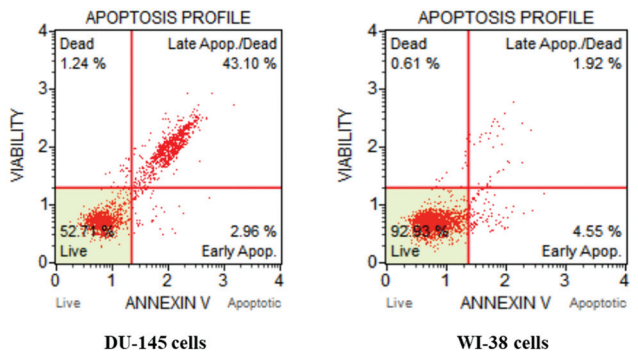

Fig. 8 Image of apoptosis analysis of DU-145 and WI-38 cells after being treated with 3.28 μg mL^{-1} CuPc (**3**) for 24 h.

3.7. Calculation results

Theoretical calculations have become so widespread because they provide excellent convenience in terms of time and money. As a result of this spread, many programs have been developed, and the most important ones are gaussian and docking programs. The biological and chemical activities of 2-(2-(3,4-dicyanophenoxy)phenyl)thiazolidine-4-carboxylic acid (**1**) and its metallophthalocyanines [ZnPc (**2**), CuPc (**3**), and CoPc (**4**)] can be compared by these methods. Recent studies have shown that the metal complexes' biological and chemical activity values were higher than those of ligand molecules.[54–56] In this study, firstly, the chemical activities of 2-(2-(3,4-dicyanophenoxy)phenyl)thiazolidine-4-carboxylic acid (**1**) and its phthalocyanine derivatives [ZnPc (**2**), CuPc (**3**), and CoPc (**4**)] are compared with the Gaussian software. Many quantum chemical parameters are obtained by the Gaussian software method. All parameters obtained from the Gaussian software are given in Table 6. The most important parameters are the HOMO (highest occupied molecular orbital) and LUMO (lowest unoccupied molecular orbital). The HOMO and LUMO values are used to compare the chemical activity of the molecules.[57] The chemical activity of the molecule having the highest HOMO value is the highest. On the other hand, the chemical activity value of the molecule having the lowest LUMO value is the highest. Using the numerical values of these two parameters, other parameters are calculated using eqn (3)–(11).

When the numerical value of the HOMO and LUMO parameters is examined, the HOMO value of ZnPc (**2**) is the

Table 6 Quantum chemical parameters for different basis sets

	E_{HOMO}	E_{LUMO}	I	A	ΔE	η	σ	χ	Pİ	ω	ε	Dipol	Energy
B3LYP/6-31g level													
Compound **1**	−6.826	−2.161	6.826	2.161	4.665	2.333	0.429	4.494	−4.494	4.329	0.231	12.866	−40 307.211
ZnPc (**2**)		−2.897	5.105	2.897	2.208	1.104	0.906	4.001	−4.001	7.250	0.138	2.850	−162 613.685
CuPc (**3**)	−5.115	−2.926	5.115	2.926	2.189	1.094	0.914	4.020	−4.020	7.384	0.135	2.818	−166 572.097
CoPc (**4**)	−5.167	−2.929	5.167	2.929	2.238	1.119	0.894	4.048	−4.048	7.323	0.137	3.161	−165 183.408
HF/6-31g level													
Compound **1**	−9.732	1.297	9.732	−1.297	11.029	5.514	0.181	4.217	−4.217	1.613	0.620	4.727	−40 106.968
ZnPc (**2**)	−5.729	−0.266	5.729	0.266	5.463	2.732	0.366	2.997	−2.997	1.644	0.608	5.645	−162 160.015
CuPc (**3**)	−6.883	1.487	6.883	−1.487	8.370	4.185	0.239	2.698	−2.698	0.870	1.150	2.019	−165 741.286
CoPc (**4**)	−7.417	0.920	7.417	−0.920	8.337	4.168	0.240	3.248	−3.248	1.266	0.790	2.613	−164 356.761
M062X/6-31g level													
Compound **1**	−8.106	−1.201	8.106	1.201	6.905	3.453	0.290	4.653	−4.653	3.136	0.319	12.253	−40 295.048
ZnPc (**2**)	−5.896	12.399	5.896	2.399	3.497	1.748	0.572	4.147	−4.147	4.919	0.203	2.670	−162 967.874
CuPc (**3**)	−5.870	−2.379	5.870	2.379	3.491	1.745	0.573	4.124	−4.124	4.873	0.205	3.300	−166 525.277
CoPc (**4**)	−5.899	−2.365	5.899	2.365	3.534	1.767	0.566	4.132	−4.132	4.831	0.207	2.639	−165 134.916

highest. If you want to sort globally by the numeric value of the HOMO: ZnPc (**2**) > CuPc (**3**) > CoPc (**4**) > **1**. If you want to sort globally by the numeric value of the LUMO: ZnPc (**2**) > CuPc (**3**) > CoPc (**4**) > **1**.

Using the optimized structures of 2-(2-(3,4-dicyanophenoxy) phenyl)thiazolidine-4-carboxylic acid (**1**) and its phthalocyanine derivatives [ZnPc (**2**), CuPc (**3**) and CoPc (**4**)], the HOMO and LUMO shapes were drawn and are given in Fig. 9. In this figure, the HOMO and LUMO orbitals can be seen to be concentrated on certain atoms. The HOMO and LUMO orbitals of ZnPc (**2**) and CoPc (**4**) are concentrated on the central atoms, but these orbitals of (**1**) and CuPc (**3**) are at the side atoms. The rightmost shapes are ESP shapes. ESP is the electrostatic charge distribution of the molecules. In these shapes, the red regions are rich in electrons, and the blue areas are electron-poor.[34]

Since all the parameters obtained as a result of Gaussian calculations are calculated from the numerical values of HOMO and LUMO parameters, they have a similar order among the other parameters.

Another method of calculating the activity of molecules is molecular docking. In molecular docking calculations, the biological activities of the molecules against cancer cells were calculated. As a result of these calculations, many parameters were obtained. The most important parameter of the obtained parameters is the *E* total energy parameter. The numerical

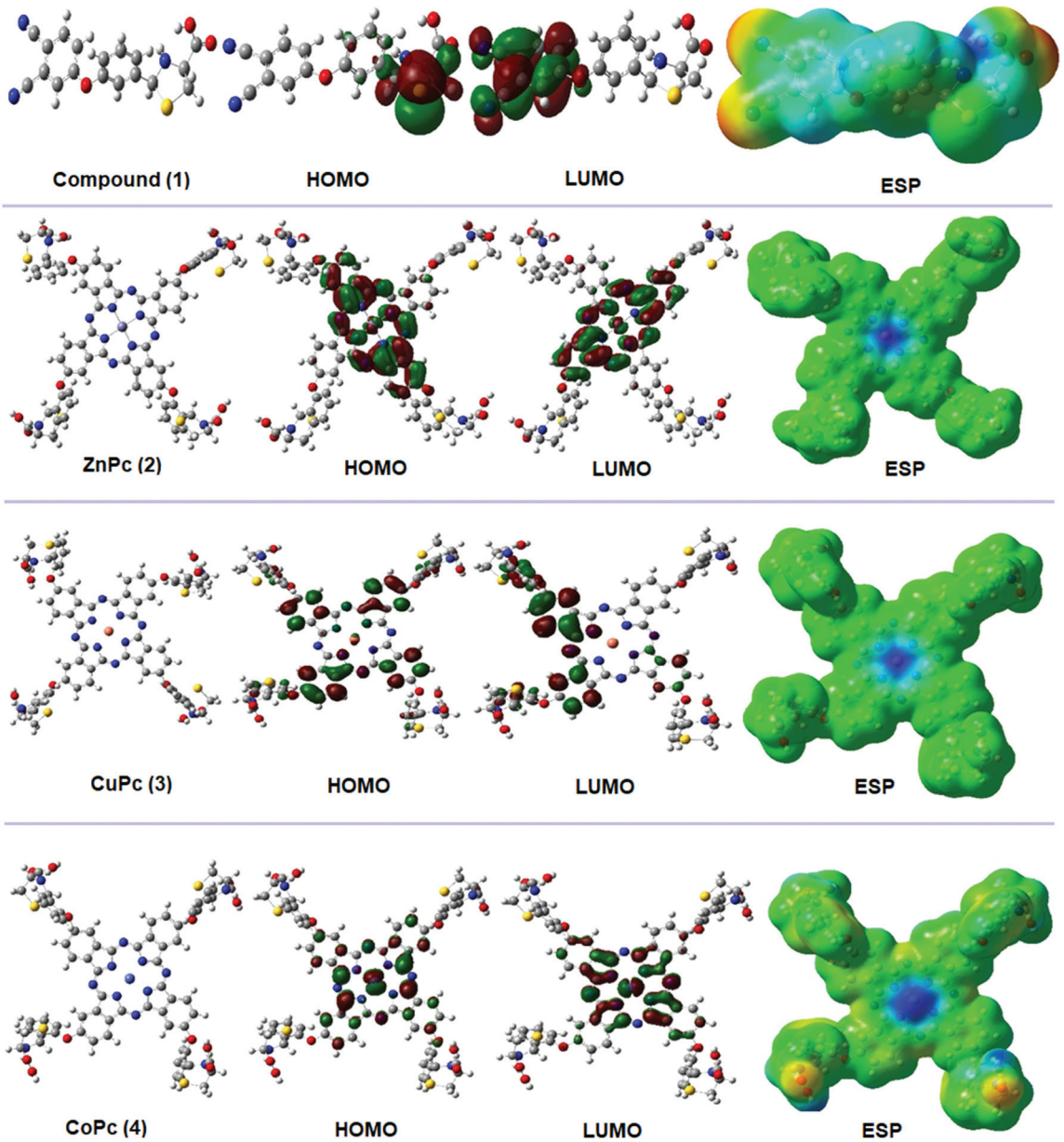

Fig. 9 HOMO, LUMO, and ESP representations of 2-(2-(3,4-dicyanophenoxy)phenyl)thiazolidine-4-carboxylic acid (**1**) and its novel metallophthalocyanines [ZnPc (**2**), CuPc (**3**) and CoPc (**4**)].

values of this parameter for compounds **1–4** are given in Table 7. In this study, the names of the cancer cells studied were respectively: the C-terminal domain of human galectin-8, whose ID was 3OJB, protease-like domain from a 2-chain hepatocyte growth factor, whose ID was 1SI5, and human glioma pathogenesis-related protein 1 in brain cancer, wherein the ID was 3Q2R. The numerical values of this parameter for compounds **1–4** are given in Table 7. The interaction of compounds **1–4** with cancer cells is shown in Fig. 10–12.

Table 7 Molecular docking *E* total energy values for the studied molecules

	Human galectin-8	Protease cancer cells	Brain cancer cells
Compound (1)	−300.30	−264.15	−264.75
ZnPc (2)	−507.07	−533.30	−538.08
CuPc (3)	−481.74	−507.11	−537.84
CoPc(4)	−500.35	−498.48	−508.59

As a result of the calculations, the biological activity values of 2-(2-(3,4-dicyanophenoxy)phenyl)thiazolidine-4-carboxylic acid (**1**) and its phthalocyanine derivatives (**2–4**) against cancer cells were compared. In these calculations, the biological activity value of ZnPc (**2**) was found to be higher than those of other molecules. The biological activity value of compound (**1**) was found to be lower than those of other molecules.[58]

According to the biological activity values of 2-(2-(3,4-dicyanophenoxy)phenyl)thiazolidine-4-carboxylic acid (**1**) and its phthalocyanine derivatives against the three cancer cells studied: ZnPc (**2**) > CuPc (**3**) > CoPc (**4**) > **1**. These values showed that the biological activity value of docking data of the phthalocyanine derivatives (**2–4**) is higher than that of 2-(2-(3,4-dicyanophenoxy)phenyl)thiazolidine-4-carboxylic acid (**1**). The biological activity values of the phthalocyanine derivatives (**2–4**) are higher than that of the phthalonitrile derivative (**1**) because the surface area of the phthalocyanine derivatives (**2–4**) is greater than that of compound (**1**).[59–61] As the surface area of the molecules increases, the contact between the mole-

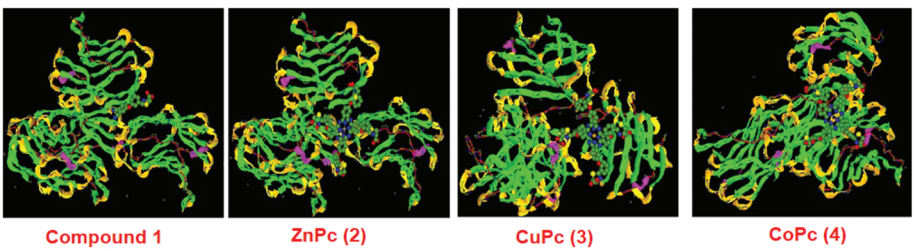

Fig. 10 Representation of the interaction of 2-(2-(3,4-dicyanophenoxy)phenyl)thiazolidine-4-carboxylic acid (**1**) and its novel metallophthalocyanines [ZnPc (**2**), CuPc (**3**), and CoPc (**4**)] with human galectin-8.

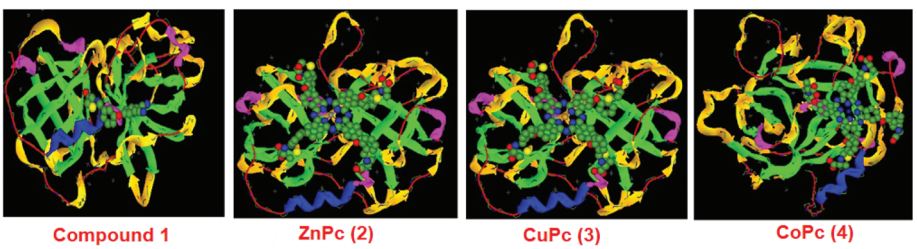

Fig. 11 Representation of the interaction of 2-(2-(3,4-dicyanophenoxy)phenyl)thiazolidine-4-carboxylic acid (**1**) and its novel metallophthalocyanines [ZnPc (**2**), CuPc (**3**), and CoPc (**4**)] with protease cancer cells.

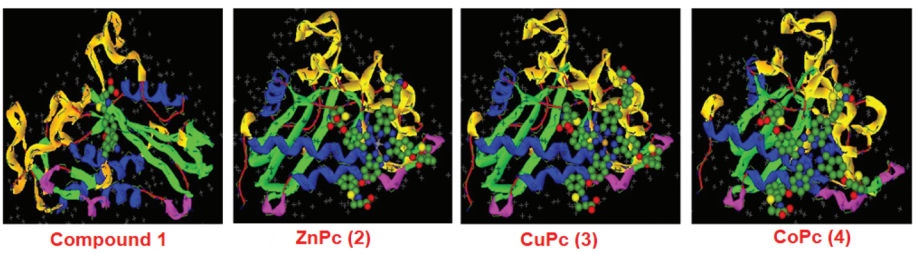

Fig. 12 Representation of the interaction of compound 2-(2-(3,4-dicyanophenoxy)phenyl)thiazolidine-4-carboxylic acid (**1**) and its novel metallophthalocyanines [ZnPc (**2**), CuPc (**3**), and CoPc (**4**)] with brain cancer cells.

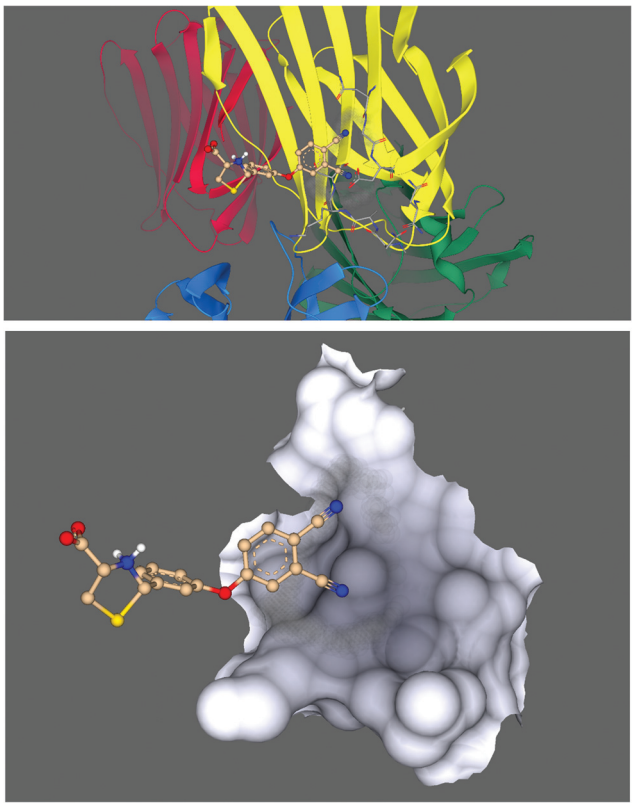

Fig. 13 Representation of the interaction of 2-(2-(3,4-dicyanophenoxy) phenyl)thiazolidine-4-carboxylic acid (**1**) with human galectin-8.

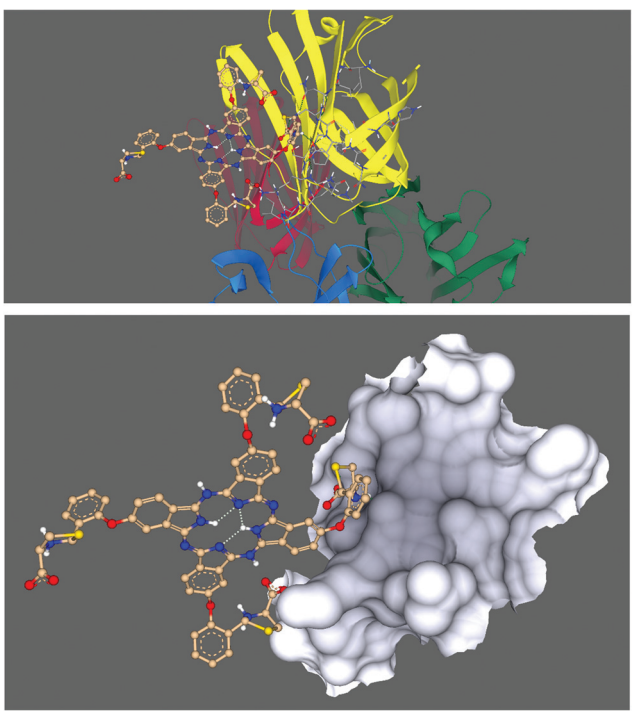

Fig. 14 Representation of the interaction of the quaternary form of 2-(2-(3,4-dicyanophenoxy)phenyl)thiazolidine-4-carboxylic acid (**1**) with human galectin-8.

Table 8 Docking parameters of molecules against human galectin-8

	Compound (**1**)	Quaternary form of (compound **1**)
hERG pIC50	3.559	2.654
log *P*	−0.520	2.970
log *S*	2.410	0.169

cule and the proteins that make up the cancer cells will increase. As a result, the interaction between the molecules and proteins will increase. These interactions are hydrogen bonds, polar and hydrophobic interactions, π–π interactions, and halogen bonds.[62] It should be well known that the effects of these interactions on the biological activity values of molecules are great.[60–62]

There are many programs to compare the biological activities of molecules. Another is the SeeSar software program.[63,64] In this program, 2-(2-(3,4-dicyanophenoxy)phenyl)thiazolidine-4-carboxylic acid (**1**) and its quaternary form were compared against human galectin-8 proteins (Fig. 13 and 14). As a result of the calculations, it was seen that the biological activity value of compound (**1**) was lower than that of its quaternary form. The parameters obtained from the calculations performed with the SeeSar 9.0 software program are given in Table 8.

When the obtained parameters were examined, it was seen that the hERG pIC50 numerical value of the quadratic form of compound (**1**) was lower. Therefore, it is understood that the biological activity value of the quaternary form of the compound (**1**) is higher. Two of the many other parameters are log *P* and log *S*. The log *S* value of the molecules studied gives information about the solubility of the molecules in water. It is an important feature in clinical trials during drug designs. This parameter provides information about the distribution of drugs used in the human body and drug delivery methods. The log *P* value is the coefficient of separation. This parameter gives information about the passage of molecules in a biological membrane.

4. Conclusion

In this paper, the thiazolidine derivative (4*R*)-2-(2-hydroxyphenyl)thiazolidine-4-carboxylic acid was synthesized and treated with 4-nitrophthalonitrile to give the phthalonitrile derivative (**1**). The novel type metallophthalocyanines (**2–4**) were obtained by the cyclotetramerization reaction of precursor phthalonitrile in the presence of related metal salts. The structure of the obtained compounds was characterized by spectroscopic methods. The aggregation behaviors and metal sensor properties of the synthesized novel type metallophthalocyanines (**2–4**) were studied by UV-Vis spectroscopy. The novel type metallophthalocyanines were found to be optically sensitive towards Ag^{+} metal ions. The fluorescence behavior of divalent ZnPc (**2**) was studied by fluorescence spectroscopy. The fluorescence quantum yield of ZnPc (**2**) was found to be 0.13. It was seen that the fluorescence quantum yield of ZnPc (**2**)

decreased compared to that of un-substituted phthalocyanine complexes. The effect of Ag^+ ions on the emission spectra of ZnPc (**2**) was also studied by fluorescence spectroscopy. The addition of Ag^+ ions to ZnPc (**2**) was caused to the quenching of fluorescence intensity. The anti-cancer activity of the novel type metallophthalocyanine derivatives (**2–4**) was studied by using six concentrations (3.125; 6.25; 12.5; 50; 75; 100 μg L^{-1}) on C6, DU-145, and WI-38 cell lines. The best activity was observed with ZnPc (**2**) in DU-145 and C6 cell lines. However, it was observed that compound CuPc (**3**) is more active when the healthy cells are considered. The total antioxidant capacity values of the novel type metallophthalocyanines (**2–4**) were found to be 5.92, 3.94, and 1.37, respectively. According to the apoptosis and cell cycle analysis of CuPc (**3**), while CuPc (**3**) had a high effect on DU145 cells, no significant effect was observed on WI-38 cells. These results suggested that CuPc (**3**) (3.28 μg L^{-1}) arrested the cells at the S-phase of the cell cycle and increased the apoptosis in DU-145 cells. The theoretical studies showed that the novel type metallophthalocyanines (**2–4**) have higher biological activity from the precursor phthalonitrile derivative 2-(2-(3,4-dicyanophenoxy)phenyl)thiazolidine-4-carboxylic acid (**1**). In both DFT and molecular docking studies, ZnPc (**2**) has the highest chemical and biological activity values. According to the obtained results from the experimental and theoretical studies, the synthesized novel type metallophthalocyanine compounds (**2–4**) might be potentially useful in the field of cancer treatment and optically sensitive to Ag^+ metal ions.

Conflicts of interest

There are no conflicts to declare.

Acknowledgements

This research was made possible by the TUBITAK ULAKBIM, High Performance and Grid Computing Center (TR-Grid e-Infrastructure).

References

1 (*a*) World Health Organization, *Cancer Key Facts*, 2018. https://www.who.int/news-room/fact-sheets/detail/cancer; (*b*) WHO report on cancer: setting priorities, investing wisely and providing care for all. Geneva: World Health Organization; 2020. Licence: CC BY-NC-SA 3.0 IGO.

2 H.-yang Fan, X.-hua Yu, Ke Wang, Yi.-jia Yin, Ya.-jie Tang, Ya-.ling Tang and X.-hua Liang, Graphene quantum dots (GQDs)-based nanomaterials for improving photodynamic therapy in cancer treatment, *Eur. J. Med. Chem.*, 2019, **182**, 111620.

3 T. V. Basova, C. Taşaltin, A. G. Gürek, M. A. Ebeoğlu, Z. Z. Öztürk and V. Ahsen, Mesomorphic phthalocyanine as chemically sensitive coatings for chemical sensors, *Sens. Actuators, B*, 2003, **96**(1–2), 70–75.

4 G. Guillaud, J. Simon and J. P. Germain, Metallophthalocyanines: gas sensors, resistors, and field-effect transistors, *Coord. Chem. Rev.*, 1998, **178**(180), 1433–1484.

5 R. Ghadari, A. Sabri, P. S. Saei, F. T. Kong and H. M. Marques, Phthalocyanine-silver nanoparticle structures for plasmon-enhanced dye-sensitized solar cells, *Sol. Energy*, 2020, **1981**, 283–294.

6 A. Suzuki, H. Okumura, Y. Yamasaki and T. Oku, Fabrication and characterization of perovskite-type solar cells using phthalocyanine complexes, *Appl. Surf. Sci.*, 2019, **48815**, 586–592.

7 E. B. Orman, A. Koca, A. R. Özkaya, I. Gürol, M. Durmus and V. Ahsen, Electrochemical, spectroelectrochemical, and electrochromic properties of lanthanide bis-phthalocyanines, *J. Electrochem. Soc.*, 2014, **161**, H422.

8 G. de la Torre, P. Vazquez, F. Agullo-Lopez and T. Torres, Phthalocyanines and related compounds: organic targets for nonlinear optical applications, *J. Mater. Chem.*, 1998, **8**, 1671–1683.

9 J. H. Zagal, S. Griveua, J. H. Silva, T. Nyokong and F. Bedioui, Metallophthalocyanine-based molecular materials as catalysts for electrochemical reactions, *Coord. Chem. Rev.*, 2010, **254**, 2755–2791.

10 L. Valli, Phthalocyanine-based Langmuir-Blodgett films as chemical sensors, *Adv. Colloid Interface Sci.*, 2005, **116**(1–3), 13–44.

11 A. T. Bilgicli, Y. Tekin, E. H. Alici, M. N. Yaraşir, G. Arabaci and M. Kandaz, α-or β-Substituted functional phthalocyanines bearing thiophen-3-ylmethanol substituents: synthesis, characterization, aggregation behavior and antioxidant activity, *J. Coord. Chem.*, 2015, **68**(22), 4102–4116.

12 A. Günsel, A. T. Bilgiçli, C. Kandemir, R. Sancak, G. Arabaci and M. N. Yarasir, Comparison of novel tetra-substituted phthalocyanines with their quaternized derivatives: Antioxidant and antibacterial properties, *Synth. Met.*, 2020, **260**, 116288.

13 R. Liang, L. Ma, L. Zhang, C. Li, W. Liu, M. Wei, *et al.*, A monomeric photosensitizer for targeted cancer therapy, *Chem. Commun.*, 2014, **50**(95), 14983–14986.

14 X. Li, B. D. Zheng, X. H. Peng, S. Z. Li, J. W. Ying, Y. Zhao, *et al.*, Phthalocyanines as medicinal photosensitizers: developments in the last five years, *Coord. Chem. Rev.*, 2019, **379**, 147–160.

15 B. Habermeyer and R. Guilard, Some activities of PorphyChem illustrated by the applications of porphyrinoids in PDT, PIT and PDI, *Photochem. Photobiol. Sci.*, 2018, **17**, 1675–1690.

16 S. Kaya, B. Tüzün, C. Kaya and I. B. Obot, Determination of corrosion inhibition effects of amino acids: quantum chemical and molecular dynamic simulation study, *J. Taiwan Inst. Chem. Eng.*, 2016, **58**, 528–535.

17 B. Tüzün and C. Kaya, Investigation of DNA-RNA Molecules for the Efficiency and Activity of Corrosion Inhibition by

DFT and Molecular Docking, *J. Bio Tribo Corros.*, 2018, **4**(4), 69.
18 Y. M. Ha, Y. J. Park, J. Y. Lee, D. Park, Y. J. Choi, E. K. Lee, *et al.*, Design, synthesis and biological evaluation of 2-(substituted phenyl)thiazolidine-4-carboxylic acid derivatives as novel tyrosinase inhibitors, *Biochimie*, 2012, **94**(2), 533–540.
19 I. Gürol, M. Durmuş, V. Ahsen and T. Nyokong, Synthesis, photophysical and photochemical properties of substituted zinc phthalocyanines, *Dalton Trans.*, 2007, **34**, 3782–3791.
20 A. Ogunsipe, Ji.-Y. Chen and T. Nyokong, Photophysical and photochemical studies of zinc(ii) phthalocyanine derivatives-effects of substituents and solvents, *New J. Chem.*, 2004, **28**, 822–827.
21 O. Erel, A novel automated direct measurement method for total antioxidant capacity using a new generation, more stable ABTS radical cation, *Clin. Biochem.*, 2004, **37**(4), 277–285.
22 R. Dennington, T. Keith and J. Millam, *GaussView, Version 6*, Semichem Inc., Shawnee Mission, KS, 2016.
23 M. J. Frisch, G. W. Trucks, H. Schlegel, G. E. Scuseria, M. A. Robb, J. R. Cheeseman, G. Scalmani, V. Barone, B. Mennucci, G. A. Petersson, H. Nakatsuji, M. Caricato, X. Li, H. P. Hratchian, A. F. Izmaylov, J. Bloino, G. Zheng, J. L. Sonnenberg, M. Hada, M. Ehara, K. Toyota, R. Fukuda, J. Hasegawa, M. Ishida, T. Nakajima, Y. Honda, O. Kitao, H. Nakai, T. Vreven, J. A. Montgomery Jr., J. E. Peralta, F. Ogliaro, M. Bearpark, J. J. Heyd, E. Brothers, K. N. Kudin, V. N. Staroverov, R. Kobayashi, J. Normand, K. Raghavachari, A. Rendell, J. C. Burant, S. S. Iyengar, J. Tomasi, M. Cossi, N. Rega, J. M. Millam, M. Klene, J. E. Knox, J. B. Cross, V. Bakken, C. Adamo, J. Jaramillo, R. Gomperts, R. E. Stratmann, O. Yazyev, A. J. Austin, R. Cammi, C. Pomelli, J. W. Ochterski, R. L. Martin, K. Morokuma, V. G. Zakrzewski, G. A. Voth, P. Salvador, J. J. Dannenberg, S. Dapprich, A. D. Daniels, O. Farkas, J. B. Foresman, J. V. Ortiz, J. Cioslowski and D. J. Fox, *Gaussian 09, Revision D.01*, Gaussian, Inc., Wallingford, CT, 2009.
24 PerkinElmer, *ChemBioDraw Ultra Version (13.0.0.3015)*, CambridgeSoft Waltham, MA, USA, 2012.
25 *Chemissan Version 4.43 package*, 2016.
26 D. Vautherin and D. M. Brink, Hartree-Fock calculations with Skyrme's interaction I. Spherical nuclei, *Phys. Rev. C: Nucl. Phys.*, 1972, **5**(3), 626.
27 A. D. Becke, Density–functional thermochemistry. III. The role of exact Exchange, *J. Chem. Phys.*, 1993, **98**(7), 5648–5652.
28 P. J. Stephens, F. J. Devlin, C. F. N. Chabalowski and M. J. Frisch, Ab initio calculation of vibrational absorption and circular dichroism spectra using density functional force fields, *J. Phys. Chem.*, 1994, **98**(45), 11623–11627.
29 K. B. Wiberg, Basis set effects on calculated geometries: 6–311 ++ G** vs. aug–cc–pVDZ, *J. Comput. Chem.*, 2004, **25**(11), 1342–1346.
30 E. G. Hohenstein, S. T. Chill and C. D. Sherrill, Assessment of the performance of the M05− 2X and M06− 2X exchange-correlation functionals for noncovalent interactions in biomolecules, *J. Chem. Theory Comput.*, 2008, **4**(12), 1996–2000.
31 S. Kaya, P. Banerjee, S. K. Saha, B. Tüzün and C. Kaya, Theoretical evaluation of some benzotriazole and phospono derivatives as aluminum corrosion inhibitors: DFT and molecular dynamics simulation approaches, *RSC Adv.*, 2016, **6**(78), 74550–74559.
32 B. Tüzün, Theoretical evaluation of six indazole derivatives as corrosion inhibitors based on DFT, *Turk. Comput. Theor. Chem.*, 2018, **2**(1), 12–22.
33 B. Tüzün, Investigation of Benzimidazole Derivates as Corrosion Inhibitor by DFT, *Cumhuriyet Sci. J.*, 2019, **40**(2), 396–405.
34 B. Tüzün, Selectivity of salicylaldoxime and its derivatives, *J. New Results Sci.*, 2014, **3**(5), 67–82.
35 L. E. Brus, A simple model for the ionization potential, electron affinity, and aqueous redox potentials of small semiconductor crystallites, *J. Chem. Phys.*, 1983, **79**(11), 5566–5571.
36 R. G. Parr and W. Yang, *Density functional theory of atoms and molecules*, Oxford University Press, Oxford, 1989.
37 Z. Bikadi and E. Hazai, Application of the PM6 semi-empirical method to modeling proteins enhances docking accuracy of AutoDock, *J. Cheminf.*, 2009, **1**, 15.
38 D. Ritchie, *Hex 8.0. 0 user manual*, 1996.
39 *LeadIT version 2.3.2*, BioSolveIT GmbH, Sankt Augustin, Germany, 2017, http://www.biosolveit.de/LeadIT.
40 N. B. McKeown, *Phthalocyanine Materials: Synthesis, Structure, and Function*, Cambridge University Press, Cambridge, 1998.
41 A. Yahyazadeh and V. Azimi, Synthesis of phthalocyanine derivatives by synergistic effect of two catalysts on zeolites under solvent conditions, *Elixir Appl. Chem.*, 2012, **49**, 9991–9993.
42 Ü. Demirbaş, D. Akyüz, B. Barut, R. Bayrak, A. Koca and H. Kantekin, Electrochemical and spectroelectrochemical properties of thiadiazole substituted metallo-phthalocyanines, *Spectrochim. Acta, Part A*, 2016, **153**, 71–78.
43 T. Fukuda and N. Kobayashi, UV-Visible, Absorption Spectroscopic Properties of Phthalocyanines and Related Macrocycles, *Handb. Porphyrin Sci.*, 2010, 1–644.
44 A. Lyubimtsev, Z. Iqbal, G. Crucius, S. Syrbu, E. S. Taraymovich, T. Ziegler and M. Hanack, Aggregation behavior and UV-vis spectra of tetra- and octaglycosylated zinc phthalocyanines, *J. Porphyrins Phthalocyanines*, 2011, **15**(01), 39–46.
45 H. Genç Bilgiçli, A. T. Bilgiçli, A. Günsel, B. Tüzün, D. Ergön, M. N. Yarasir and M. Zengin, Turn–on fluorescent probe for Zn^{2+} ions based on thiazolidine derivative, *Appl. Organomet. Chem.*, 2020, e5624.
46 A. T. Bilgicli, A. Gunsel, M. Kandaz and A. R. Ozkaya, Highly selective thioalcohol modified phthalocyanine sensors for Ag(i) and Pd(ii) based on target induced J- and H-type aggregations: synthesis, electrochemistry and peripheral metal ion binding studies, *Dalton Trans.*, 2012, **41**, 7047–7056.

47 A. Günsel, A. T. Bilgiçli, B. Tüzün, H. Pişkin, M. N. Yarasir and B. Gündüz, Optoelectronic parameters of peripherally tetra-substituted copper(II) phthalocyanines and fabrication of a photoconductive diode for various conditions, *New J. Chem.*, 2020, **44**(2), 369–380.
48 A. Ogunsipe, J.-Y. Chen and T. Nyokong, Photophysical and photochemical studies of zinc(II) phthalocyanine derivatives-effects of substituents and solvents, *New J. Chem.*, 2004, **28**(7), 822–827.
49 S. Demir, Y. Aliyazicioglu, I. Turan, S. Misir, A. Mentese, *et al.*, Antiproliferative and proapoptotic activity of Turkish propolis on human lung cancer cell line, *Nutr. Cancer*, 2016, **68**, 165–172.
50 Z. Li, H. Yan, Q. Sang, K. Wang, Q. He, Y. Wang and F. Hu, Antitumor activity of Chinese propolis in human breast cancer MCF-7 and MDA-MB-231 cells, *J. Evidence-Based Complementary Altern. Med.*, 2014, 1–11.
51 R. J. Duronio and Y. Xiong, Signaling Pathways that Control Cell Proliferation, *Cold Spring Harbor Perspect. Biol.*, 2013, **5**(3), a008904.
52 J. M. Skotheim, S. DiTalia, E.D. Siggia, *et al.*, Positive feedback of G1 cyclins ensures coherent cell cycle entry, *Nature*, 2008, **454**, 291–296.
53 S. Elmore, Apoptosis: A Review of Programmed Cell Death., *Toxicol. Pathol.*, 2007, **35**(4), 495–516.
54 I. Ali, W. A. Wani, K. Saleem and M. F. Hseih, Design and synthesis of thalidomide based dithiocarbamate Cu(II), Ni (II) and Ru(III) complexes as anticancer agents, *Polyhedron*, 2013, **56**, 134–143.
55 K. Saleem, W. A. Wani, A. Haque, M. N. Lone, M. F. Hsieh, M. A. Jairajpuri and I. Ali, Synthesis, DNA binding, hemolysis assays and anticancer studies of copper(II), nickel(II) and iron(III) complexes of a pyrazoline-based ligand, *Future Med. Chem.*, 2013, **5**(2), 135–146.
56 I. Ali, W. A. Wani, K. Saleem and M. F. Hsieh, Anticancer metallodrugs of glutamic acid sulphonamides: in silico, DNA binding, hemolysis and anticancer studies, *RSC Adv.*, 2014, **4**(56), 29629–29641.
57 J. I. Aihara, Reduced HOMO− LUMO gap as an index of kinetic stability for polycyclic aromatic hydrocarbons, *J. Phys. Chem. A*, 1999, **103**(37), 7487–7495.
58 B. Tüzün, Investigation of pyrazolyl derivatives schiff base ligands and their metal complexes used as anticancer drug, *Spectrochim. Acta, Part A*, 2019, 117663.
59 G. Mamedova, A. Mahmudova, S. Mamedov, Y. Erden, P. Taslimi, B. Tüzün, R. Tas, V. Farzaliyev, A. Sujayev, S. H. Alwasel and İ. Gulçin, Novel tribenzylaminobenzolsulphonylimine based on their pyrazine and pyridazines: Synthesis, characterization, antidiabetic, anticancer, anticholinergic, and molecular docking studies, *Bioorg. Chem.*, 2019, **93**, 103313.
60 B. Tüzün and E. Saripinar, Molecular docking and 4D-QSAR model of methanone derivatives by electron conformational-genetic algorithm method, *J. Iran. Chem. Soc.*, 2019, 1–16.
61 A. Günsel, A. Kobyaoğlu, A. T. Bilgiçli, B. Tüzün, B. Tosun, G. Arabaci and M. N. Yarasir, Novel biologically active metallophthalocyanines as promising antioxidant-antibacterial agents: Synthesis, characterization and computational properties, *J. Mol. Struct.*, 2020, **1200**, 127127.
62 H. G. Bilgicli, P. Taslimi, B. Akyuz, B. Tuzun and İ. Gulcin, synthesis, characterization, biological evaluation, and molecular docking studies of some piperonyl–based 4−thiazolidinone derivatives, *Arch. Pharm.*, 2019, **353**(1), 1900304.
63 M. Imber, V. V. Loi, S. Reznikov, V. N. Fritsch, A. J. Pietrzyk-Brzezinska, J. Prehn, J. Hamilton, C. Wahl, M. C. Bronowska, K. Agnieszka and H. Antelmann, The aldehyde dehydrogenase AldA contributes to the hypochlorite defense and is redox-controlled by protein S-bacillithiolation in Staphylococcus aureus, *Redox Biol.*, 2018, **15**, 557–568.
64 I. Sagud, I. Skoric, D. Vuk, A. Ratkovic and F. Burcul, Acetyl-and butyrylcholinesterase inhibitory activity of selected photochemically synthesized polycycles, *Turk. J. Chem.*, 2019, **43**(4), 1170–1182.

